

**RETRO-COMMISSIONING OF A HEAT SOURCE SYSTEM IN A
DISTRICT HEATING AND COOLING SYSTEM**

Eikichi Ono^{1*}, Harunori Yoshida², Fulin Wang³

¹KAJIMA Corporation, Tokyo 107-8502, Japan,

²Department of Architecture, Okayama University of Science, Okayama, Japan,

³Department of Building Science, Tsinghua University, Beijing, China

ABSTRACT

To improve the energy performance of a district heating and cooling (DHC) plant, the expected performance of the plant was studied using simulations based on mathematical models. A model of the entire heat source system with an embedded module that automatically determines the on/off status of heat source equipment using cooling/heating loads was developed and validated using measured actual performance data. The mean error between the simulated and measured total energy consumption was 4.2%. Using the developed model, four proposals for improving the plant operation were simulated to determine potential energy savings. The simulation results show that the four proposals, reducing pipe resistance, optimization of chiller subsystem, improving the operation of chilled-hot water switchover thermal storage tanks, and optimizing the operational control of an external thermal storage tank, can reduce the energy

consumption of the thermal storage pumps by 24%, chiller subsystem by 1.4%, and energy consumption and costs of the entire plant by 6% and 2.7%, respectively. If all of four proposals were applied, total power consumption and energy costs could be reduced by 11.0% and 8.2%, respectively.

KEYWORDS

Retro-commissioning, optimization, district heating and cooling plant, energy conservation, simulation

INTRODUCTION

In recent years, environmental issues, including global warming, have gained attention throughout the world. In order to reduce carbon dioxide (CO₂) emissions and achieve sustainable development, efficient energy use has become increasingly important. District Heating and Cooling (DHC) systems are an attractive option for urban areas due to their higher energy efficiency and greater resulting reduction in

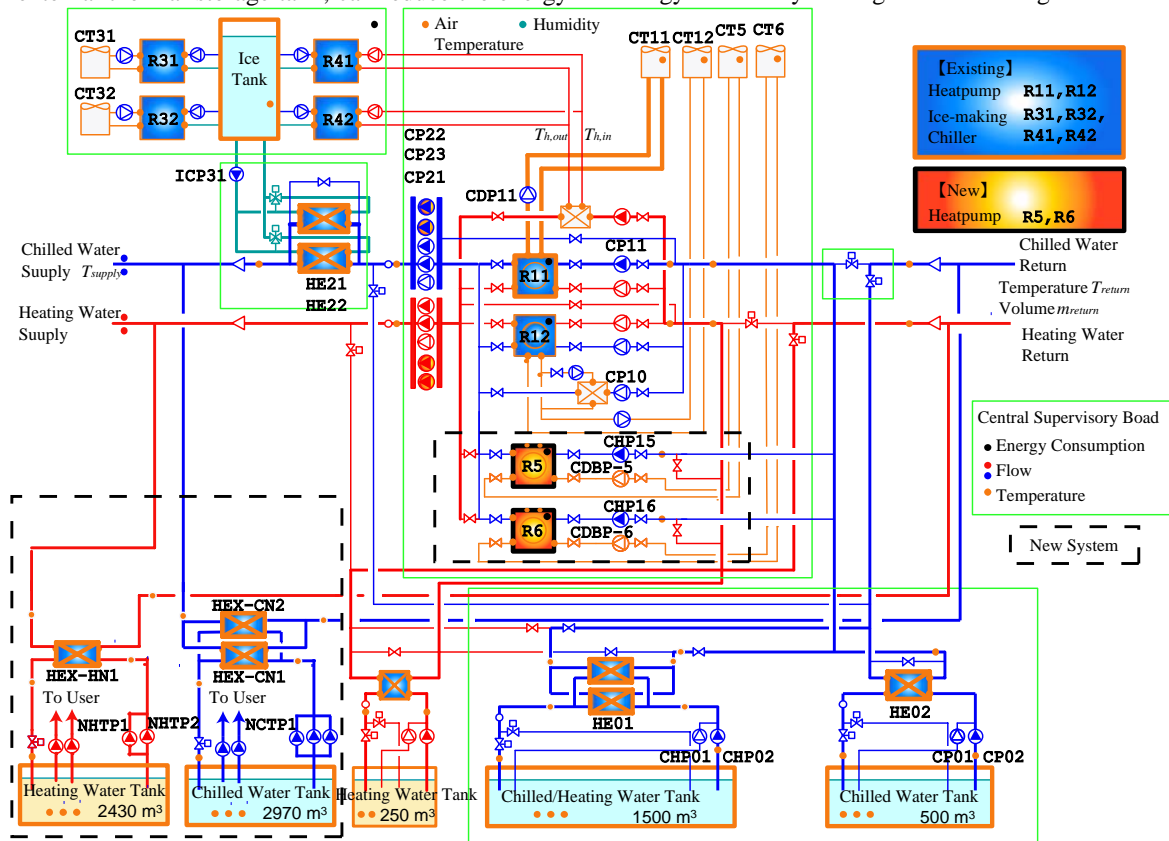


Figure 1: Heat source system diagram

harmful waste emissions than traditional heating and cooling systems. However, the Coefficient of Performance (COP) of DHC systems is often reported to be less than one because many DHC systems are not being operated properly. The effective and efficient operation of DHC systems requires the development and use of an enhanced operation mode, which improves energy efficiency while fulfilling required heating and cooling demands. The purpose of the present research is to optimize the operation of an existing DHC plant during the retro-commissioning process. In a previous study, the authors had reported on the construction of a system simulation model and proposed four methods for improving DHC system operation, i.e., optimizing the cooling water temperature of a centrifugal chiller; automating the control of the primary chilled water flow rate; changing the set point temperature of the chilled water supply; and changing the opening of the bypass valve for the ice thermal discharge heat exchanger (Shingu et al., 2008). In the present paper, the results of optimizing the operation of a thermal storage tank and newly-introduced screw heat pumps are reported.

PROFILE OF THE PLANT

The DHC plant in the current study, located in Osaka, Japan, has served two buildings (one office building and one building with hotel rooms and leisure facilities) since November 1992. In 2007, the DHC plant was expanded to serve another office building. Figure 1 shows the system diagram of the plant. Existing and newly introduced equipment is shown in different colors. Table 1 presents detailed information on the main plant equipment.

The present sequence of operating heat source equipment is R5, R6, R11, and R12. Ice chillers are operated according to heating demand with a normal sequence of R41, R42, R31, and R32.

MODELING OF HEAT SOURCE SYSTEM

Modeling and validation of heat source equipment

The heat source equipment modeling and validation process was conducted as follows: 1) Development of a model using the characteristic curve provided by

manufacturers: 2) Comparison of the model-simulated data with the specification data to check model accuracy; 3) Derivation of a compensation coefficient from measured data to revise the model-calculated data for the purpose of simulating the actual performance of the DHC plant. The models are described in detail in the authors' previous paper (Shingu et al., 2008).

Modeling and validation of the heat source system

The heat source equipment models described in the previous section were connected to construct the complete heat source system model. The accuracy of the system simulation was then validated. The 180-day simulation period was from March 5th to October 31st, with a simulation interval of 10 minutes. The actual on/off status of the heat source equipment and actual chilled water flow rates to each heat pump were used to check the simulation accuracy of the system model. The average simulation error was 4.1% and the Root Mean Square Error (RMSE) was 8.7%. Figure 2 shows the comparison of simulated and measured total plant power consumption. The simulation interval is ten minutes and the power consumption results are accumulated every six times to get the values in kWh which are plotted in the figure to compare with the real power consumption. The summed simulated and measured power consumption of each component is shown in Table 2. The simulation error for chillers, which consume the largest amount of energy, impacted the total simulation accuracy. The simulation error for chillers resulted from the use of a set point chilled water temperature instead of an actual chilled water temperature. Consequently, the simulation error is caused by the following two operational conditions.

- 1) During actual operation, the chilled water outlet temperature of R5, R6 and R11 is set at 5 °C, and that of R12 is set at 5.5 °C. However, the measured temperature is not constant, but fluctuates around the set point. In the simulation, the average

Table 2: Integral power consumption

	Whole system	Chillers	Cooling towers	Pumps
Measured [MWh]	3804	2543	133	1129
Simulated [MWh]	3649	2384	139	1126
Average error [%]	4.1	6.3	-4.9	0.2

Table 1: Heat source equipment

	Heat Source Equipment	Name	Capacity (Chiller: RT, Tank: m ³)	Number
Existing	Two-centrifugal-compressor heat pump	R11	700	1
	Centrifugal heat pump with heat recovery	R12	700	1
	Ice chiller with heat recovery	R41, R42	37	1, 1
	Air source screw ice chiller	R31, R32	75	1, 1
	Chilled water tank	-	500	1
	Chilled-heat water switchover tank	-	1500	1
	Heat water tank	-	250	1
	Ice thermal storage tank	-	150	1
Newly introduced	Three-screw-compressor heat pump	R5, R6	450	1,1

measured temperature, which is a constant value, is input into the model, thereby causing the error.

- 2) In the simulation, the discharge temperature of the water thermal storage tank is set at 9 °C. However, during actual operation the temperature is manually set between 8 °C and 9 °C, an inconsistency that contributes to the error.

The first condition occurs because of the chiller control problem or the bias of the temperature sensors. The second condition appears because the rule of changing the set point is not established, making it difficult for a simulation to match actual operation.

However, the error is caused by the difference between the actual operation and simulation input, therefore, the simulation accuracy is sufficiently acceptable to use the model to search for optimal operation.

DEVELOPMENT OF AUTOMATED ON/OFF STATUS DETERMINATION TOOL

Automated determination tool of ON/OFF status

The automated determination tool of on/off status automatically determines the whether heat source equipment is functioning or not operating based on the operation priority order, the threshold of starting/stopping the heat source machine, and the time series for the heating/cooling load or thermal level of thermal storage tank. During the non-thermal-storage period, the time serial heating/cooling load is compared to the load threshold and the necessary heat source

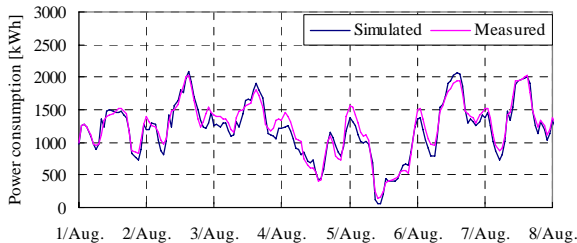


Figure 2: Power consumption (model validation)

machines are selected. During the thermal storage period, the target thermal level designated for storage is used to determine which heat source machines should operate at the beginning of the thermal storage period. Then, the thermal level in the storage tank is compared to the threshold level to decide which heat source machine should cease operation based on a pre-determined priority order. Figure 3 shows the flow of the algorithm for determining the on/off status during the thermal storage period.

Standard model

During actual operation, human operators manually operate the heat source system, but the rules of operation are not uniform or clear. The operation methods differ at different outdoor air temperatures, load conditions, and for different operators. Consequently, the measured data are not sufficiently consistent to be used as a comparison base to evaluate the simulated performance of the operation proposals. Thus, a “standard system model,” which imitates actual operation as closely as possible, was developed to serve as an acceptable comparison base. The standard model is based on the actual operation method from which the ambiguity of manual operation is removed. In the standard model, the on/off status of heat source equipment is determined using the tool mentioned in the previous section and the primary chilled water flow rates are calculated according to the control algorithm instead of using measured data. The standard model accuracy is then checked by comparing the results to

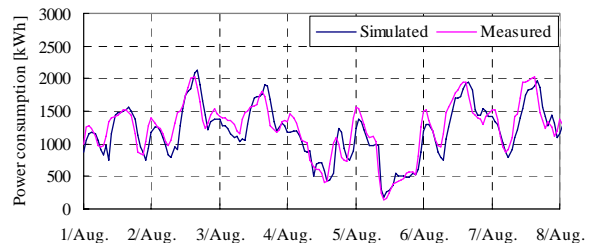


Figure 4: Power consumption (standard model)

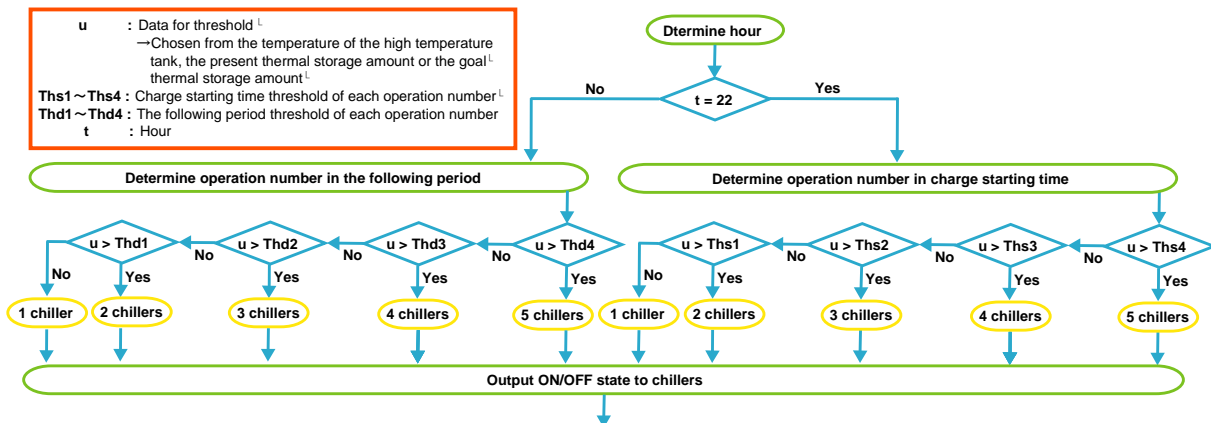


Figure 3: Algorithm for determining ON/OFF status during charge period

measured data. The average simulation error of total energy consumption is 2.8% and RMSE is 13.5%. The time series comparison of the simulated and measured total plant power consumption is shown in Figure 4. The simulation accuracy shows that this model reflects actual operation accurately, and can be used as a comparison base to evaluate the proposals discussed in the following sections.

RETRO-COMMISSIONING OF THE DHC PLANT

The retro-commissioning was conducted to verify the performance of the DHC plant, for which commissioning had never previously been conducted, and to propose performance improvement methods. The retro-commissioning process was divided into three categories, individual machines, subsystems and whole system, and performance verification of the proposed performance improvement methods was conducted for each category. The system performance aspects studied in the current research are shown in Figure 5. In addition, the study evaluated the power consumption and energy costs of the thermal storage system. The energy costs were calculated as follows.

$$C_d = E_d \cdot P_d \quad (1)$$

$$C_n = (E_n - E_{np})(P_n \cdot \eta + P_d(1 - \eta)) + E_{np} \cdot P_d \quad (2)$$

Where, η equals 0.88, which indicates that the power consumed by the thermal storage machines is 88% of the total power consumption. The nighttime energy cost rate can be applied to this calculation. In contrast, the cost of power consumed by pumps at the newly serviced building cannot reflect nighttime energy cost rates.

Performance verification of newly-introduced chillers

The newly-introduced heat pumps, R5 and R6, have higher performance efficiency at partial load than at full

load. Figure 6 shows the specification curve for the chillers. The highest COP appears at a load factor of 40%. The performance verification of the chillers was conducted to determine whether or not the machine performance conforms to the specification curve. Figures 7 and 8 show the measured COP for the chillers and subsystem, which includes chiller, cooling tower, chilled water pump and cooling water pump. These figures illustrate that: 1) the measured COP is lower than the specification curve; 2) the measured COP of R6 is higher than that of R5; and 3) the COP for a partial load is not necessarily higher than for a full load when the performance is evaluated based on the subsystem COP. The reasons for observations 1) and 2) are not clear; however they may result from the scattering of the machine performance. The reason for observation 3) is that the actual partial load performance is lower than the specification curve. Furthermore, the subsystem COP at partial load becomes smaller because the proportion of auxiliary machines' power consumption becomes larger at the partial load. Consequently, the partial-load operation of chillers is not an optimal operating condition.

Reducing pipe resistance

Currently, the valves at the outlets of pumps of NCTP1, 2 and 3, which are in the newly serviced building, are opened to 30%, generating a large amount of resistance from the valves that must be overcome by the pumps. This operating condition is necessary because the pump design head is larger than actual pipe

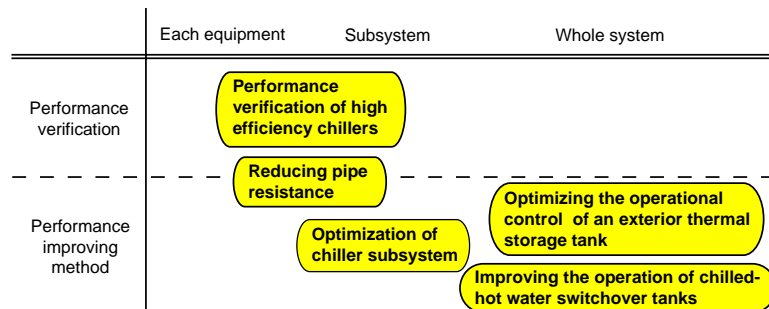


Figure 5: The orientation of studies conducted in this research

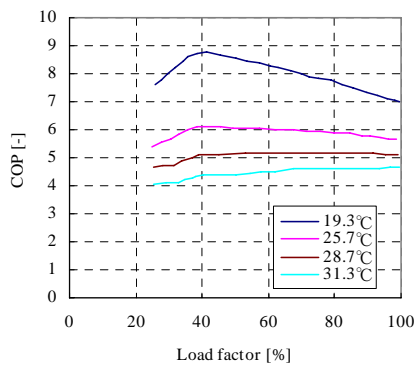


Figure 6: The specification curve of R5 and R6

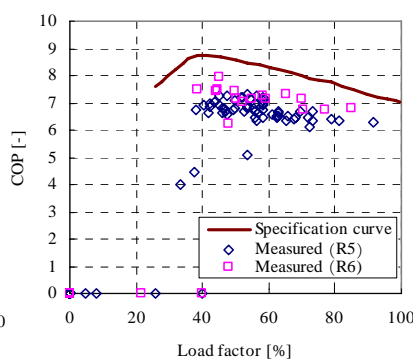


Figure 7: The measured COP of chillers

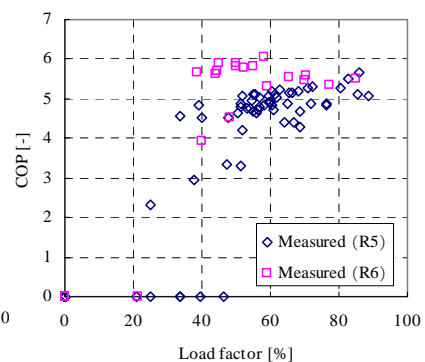


Figure 8: The measured COP of subsystem

resistance and if the pumps were operated with a fully opened valve, problems such as an excessive flow rate and unstable operation would occur. To address this inefficiency, an operation method that is more energy-efficient considering both safety and stability was developed.

First, an experiment was conducted to evaluate operation of the pumps with fully opened valves to verify the actual pump performance. Based on the experimental data, the model-based characteristic curves of power consumption for fully opened valves and 30% opened valves were developed as shown in Figure 9. Under the proposed operation with a fully opened valve, certain water flow rates cannot be achieved through pump control (“impossible water flow rate”) due to the available pump flow rates. However, the water temperature of the thermal storage tank can be controlled as required because the water temperature and primary water flow rate at the heat exchanger is automatically controlled; therefore, the impossible water flow rates do not interfere with system operation.

Second, the proposed operation was verified using simulation. The proposed operation can reduce pump energy consumption by 24.0%. To verify the influence of the impossible water flow rate range, the number of hours that the starting tank temperature of the proposed operation exceeds that of the standard model was calculated (Table 4). The starting tank temperature was 0.1°C higher than the standard model 1.4% of the time during all simulation periods, indicating that the influence of the impossible water flow rate is negligible.

Optimization of chiller subsystem

The cooling water pump, the rotation of the cooling tower fan, and the rotational speed of the heat pumps in R5 and R6 are controlled using a frequency inverter based on the number of chiller compressors that are running. The rotational speeds at the minimum power consumption level of the subsystem, which includes chillers, cooling water pumps and a cooling tower fan, were searched hourly using an optimizing method (Zhang 2008). The proposed improved control method is based on the optimization results.

The subsystems of heat pump R5 and R6 were optimized. The results of heat pump R5 are evaluated as an example. Table 5 shows the monthly reduction rate in the subsystem power consumption. The optimal control level is shown to reduce the summed power consumption of the total simulation period by 1.4%. The results also show that setting the cooling water pump to run at low rotational speed while running the

cooling tower fan at high speed is more efficient. The results also show that the differences between the optimized and measured data were small, which means that the present control is similar to the optimal control.

Based on the results of the optimization, the following two improved control methods were proposed.

(a) Regression model

Figure 10 and 11 show the correlation of the optimal rotation and cooling load. The optimal rotations of the cooling water pump change according to cooling load and wet bulb temperatures, and the optimal rotations of the cooling tower fan change based on cooling load. Therefore, the following regression equation is used as a simple estimation method of the optimal rotation.

$$I_p = a_1 T_{wb} + a_2 Q + a_3 T_{wb} Q + a_4 \quad (3)$$

$$I_c = b_1 Q^2 + b_2 Q + b_3 \quad (4)$$

The RMSE between the values calculated using the regression equations and optimal rotations of the cooling water pump and cooling tower fan are 2.7% and

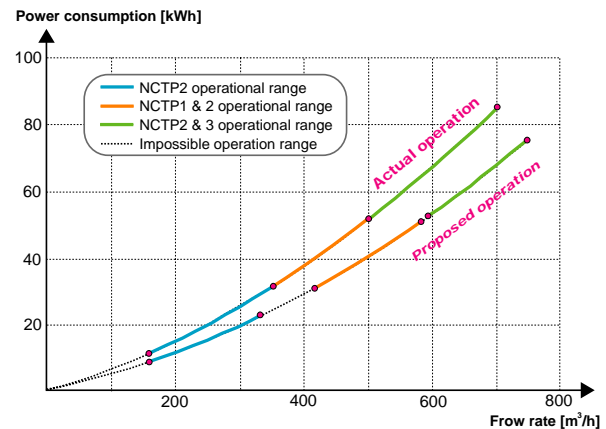


Figure 9: The characteristics of power consumption relative to water flow rate

Table 4: Verification of the starting tank temperature

	Over 0.5°C	Over 0.3°C	Over 0.1°C
Hours [h]	5	9	62
Proportion to all period [%]	0.1	0.2	1.4

Table 5: The rates of reduced chiller subsystem power consumption

	Apr	May	Jun	Jul	Aug	Sep	Total
Optimization [%]	3.46	1.78	1.46	1.25	1.04	1.33	1.40
Regression model [%]	3.01	1.34	1.08	1.04	0.86	1.05	1.11
Optimal set point [%]	1.61	1.07	0.99	0.88	0.70	0.82	0.90

Table 6: The present and optimal rotation rates for operation of different number of compressor units

		1 compressor	2 compressors	3 compressors
Cooling pump [-]	Present	0.50	0.65	0.86
	Optimal	0.44	0.57	0.76
Cooling tower's fan [-]	Present	0.40	0.60	0.80
	Optimal	0.38	0.61	0.87

3.0%, respectively. The effects of the control using this regression model were checked and the results are shown in Table 5. Using this control method, power consumption over the total simulation period is reduced by 1.1%.

(b) Optimal set point

The set point of the present control is improved based on the average optimal rotation. Table 6 shows the present and optimal set points, and Table 5 shows the reduction in the power consumption rate at the optimal set points. The improved set points can reduce power consumption over the total simulation period by 0.9%.

Improving the operation of chilled-hot water switchover tanks

The DHC system has four thermal storage tanks. The largest thermal storage tank is used to store chilled water during the summer and hot water during the winter. Therefore, the switchover period between the chilled and hot water is very important. In this section, improved operation of the thermal storage tanks is proposed based on the evaluation of the switchover period.

Under the present operating conditions, one of the high efficiency heat pumps, R5 or R6, is operated in heating mode. However, this operation is considered to be improper because the cooling load is much larger than the heating load during the moderate season. Although heat pumps R11 or R12 can be operated in heating mode, they are not operated during actual operation for the following two reasons. 1) Only one of the four thermal storage tanks is used to store hot water in the moderate seasons. Because the capacity of hot water tank is small, R11 or R12 cannot be operated because their capacities are too large for the stored hot water in the tank. 2) The human operators assume that the operation of R5 and R6, one in cooling mode and one in heating mode, is more

efficient because their COP is higher at partial load conditions.

To resolve the obstacles related to operating R11 or R12 in the heating mode, 1) the chilled-hot water switchover tank can be operated in hot water mode and 2) R11 can be operated in heat recovery mode.

The proposed operation was simulated for March 5th to October 31st and the switchover period from chilled to hot water storage was studied. The chilled-hot water switchover tank is used in chilled water mode during the period when the chilled water supply temperature is higher than the standard model, a condition that implies that the cooling load is large and the chilled-hot water tank needs to switch to chilled water mode. Figure 12 shows the correlation between the daily summed cooling load and the number of degrees the chilled water supply temperature is above standard operation temperature. The results show that the chilled water supply temperature will be higher than standard operation temperature if the load rises above 300 GJ. Therefore, the chilled-hot water tank needs to operate in chilled water mode from approximately the end of July to the end of September, when the cooling load exceeds 300 GJ on most days.

This operating rule was applied to the simulation. Table 7 shows the rate of reduced power consumption and energy costs for the whole system. Both energy consumption and costs can be reduced by approximately 6% over six months by applying this operating rule.

Optimizing the operational control of an external thermal storage tank

The newly serviced building does not directly receive the chilled and hot water from the DHC plant. The new building has two large thermal storage tanks to store

Figure 7: The rate of reduced power consumption and energy costs

	May	Jun	Jul	Aug	Sep	Oct	Total
Power consumption [%]	25.2	14.2	4.0	0.0	0.1	11.5	6.3
Energy cost [%]	25.3	13.1	3.1	0.0	0.1	10.9	5.6

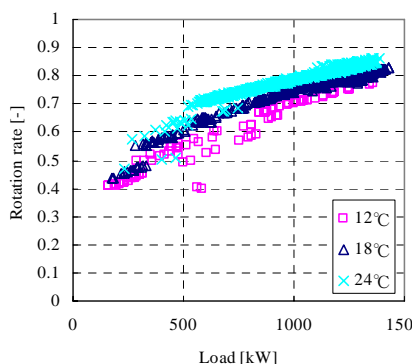


Figure 10: The correlation of the pump rotation to load at each wet bulb temperature

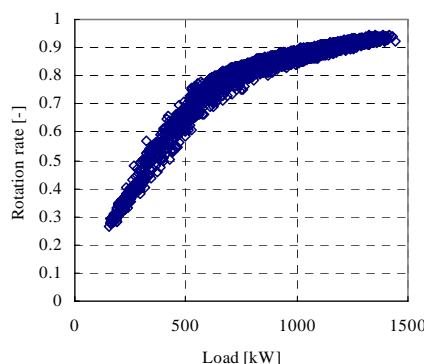


Figure 11: The correlation of the cooling tower's fan rotation to load

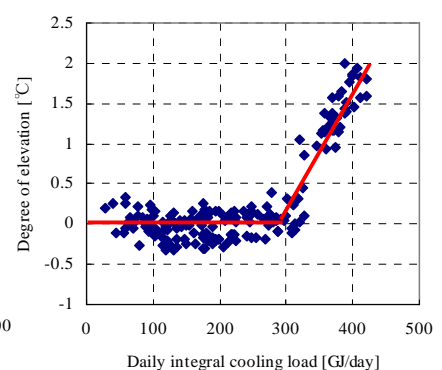


Figure 12: The correlation of the daily summed cooling load to the degree of temperature elevation

chilled and hot water. The stored chilled and hot water, respectively cools and heats the water stored in the tanks through heat exchangers. Figure 13 shows the thermal storage tank system diagram. Under present operations, the secondary water flow rate m_2 and the temperature difference dT between the primary water inlet and secondary water outlet are controlled automatically. The control rule applied to the set points for m_2 and dT is not clearly determined and the human operators determine them manually. In this section, we aim to optimize the set points for m_2 and dT .

(a) Case study of controlled objects

Case studies were conducted with the set points for m_2 set at {200, 300, 400, 500, 600} m³/h, dT set at {0.3, 0.6, 0.9, 1.2, 1.5} °C, and T_f set at {6, 7} °C. Where, T_f is the temperature at which thermal storage ends. Furthermore, dT was set separately for daytime and nighttime. In total, 250 cases were simulated. The results show that operation using weekly optimal set points can reduce the total power consumption and energy costs by 3.3% and 1.2%, respectively. Furthermore, the correlation between the optimal set points for outdoor air temperature and the heat load was analyzed, but a clear correlation could not be found so a rule for actual operation is not available.

(b) Optimization of controlled objects

The controlled set points were optimized at the instant steady state. The objective function for this optimization is shown in Equation 5.

$$\max(V = Q_s - E_s) \quad (5)$$

This equation was determined to maximize the thermal storage amount and minimize the total power consumption. Where, E includes the energy

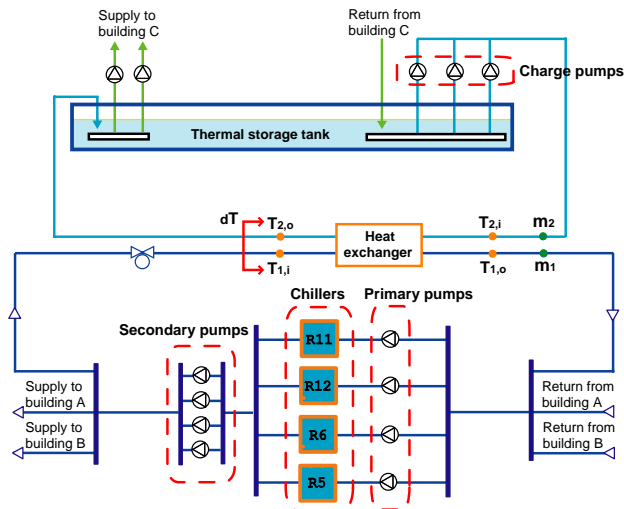


Figure 13: System diagram of the thermal storage tank

consumption of chillers, primary pumps, secondary pumps, and thermal storage pumps. Furthermore, this equipment consists of several duplicate machines and the number of components operating is controlled according to load. For the purpose of solving the optimization problem, one virtual equivalent machine is used to simulate the performance of several identical units. Without the use of a virtual equivalent machine, the evaluation function becomes discontinuous or not smooth at the switchover point of the operation number and the ideal optimal point cannot be found. A regression using quadratic equations of the measured water flow rates and cooling loads is performed for the power consumption model of the pump and chiller, respectively. The simulation errors between the simulated and measured power consumption are shown in Table 8.

The model is then used to identify the optimal solution. The optimal points are captured at the same thermal level stored in the tank at different $T_{2,i}$, the temperature of water at the end of the tank. Figure 14 shows the change in evaluation variable V accompanying the water flow rate m_2 at each $T_{2,i}$. The optimal points are marked in the figure with red diamonds. However, the optimal set point for m_2 is the maximum flow rate when $T_{2,i}$ is lower than 11 °C because the total capacity of the thermal storage pumps is approximately 900 m³/h.

The performance of the thermal storage pumps is simulated when the optimal set points are applied to the operation. Control of the hourly thermal storage amount is necessary for the optimization of the thermal storage operation during the nighttime period, which is set as 10 hours. Figure 15 shows the control method for hourly thermal storage amounts. The operations were simulated with six different maximum thermal storage rates, from 9000 MJ/h to 14000 MJ/h per 1000 MJ/h, to find the optimal maximum daily thermal storage rate. The results indicate that more energy can be conserved if the maximum thermal storage rate is set lower. However, if the thermal storage rate is set too low, the

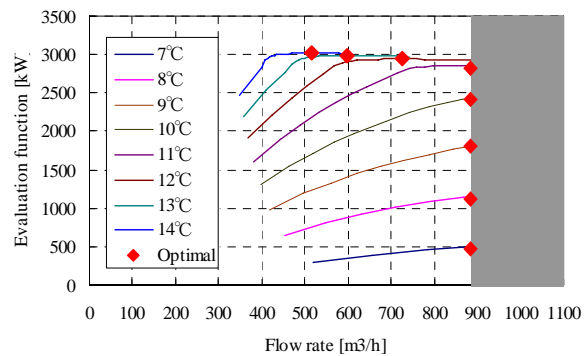


Figure 14: Correlation of m_2 and V for each $T_{2,i}$

target thermal storage volume cannot be met. Therefore, rate should be set at the lowest thermal storage rate that satisfies the target. System operation using the daily optimal thermal storage rates can reduce the total power consumption by 2.7%.

Sum of the conducted studies

Table 9 shows the total effect of the four proposals as applied to the DHC plant. The total power consumption and energy cost can be reduced by 11.0% and 8.2%, respectively, over six months.

CONCLUSIONS

A retro-commission study on the heat source system of a DHC plant was conducted to detect deficiencies and to identify optimal operating conditions using a simulation. The simulation model for the heat source system was developed to check equipment performance and to find optimal operating conditions and check potential energy savings.

1) The performance of the entire heat source system, including the newly installed heat source equipment was simulated. The average simulated error of the total energy consumption of the plant was 4.1% of its measured value, and the RMSE was 8.7%. This indicates that the simulation is sufficiently accurate to be used to identify optimal operating methods.

2) A tool was developed that automatically determines the on/off status of heat source equipment during both, thermal storage and discharge periods.

3) The performance of newly installed chillers with the highest COP at partial load conditions was verified. The results show the operation of these chillers at partial load is not a good practice.

4) The performance results of four operation-optimizing proposals were checked. If all of four proposals were applied, the power consumption and energy costs could be reduced by 11.0% and 8.2%, respectively.

REFERENCES

Yoshida H.: Optimal Operation Method of Heat Source System Based on Probability Distribution of Air-Conditioning Load, *Proceedings of the Annual Meeting of the Society of Heating, Air-conditioning and Sanitary Engineers (SHASE)*, No. H2, pp. 665, 1990.

Shingu H., Nakajima R., Yoshida H., Wang F.: Retro-Commissioning and Improvement for District Heating and Cooling System Using Simulation, *International Conference of Enhanced Building Operation, Shenzhen*, Vol. 6-6-6, November, 2006.

Shingu H., Yoshida H., Wang F., Ono E.: Preliminary Retro-Commissioning Study on Optimal Operation for the Heat Source System of District Heating/Cooling Plant, *International Conference of Enhanced Building Operation, Berlin*, October, 2008.

Shingu H., Nakajima R., Yoshida H., Wang F.: The Retro-Commissioning and Operation Improving Schemes for the Heat Source of a District Heating and Cooling System, *Annual Meeting of SHASE*, Kinki, pp. 93, 2006.

Zhang Z., Yoshida H., Miyata M., Shingu H., Yamashita T., Tashiro H.: Research on Optimal Operation and Design of Cooling Heat Source Equipment by Simulation, *Annual Meeting of SHASE*, 2008.

NOMENCLATURE

- C_d : Daytime energy cost, [yen]
- C_n : Nighttime energy cost, [yen]
- E_s : Total power consumption of all equipment used for thermal storage, [kW]
- E_d : Daytime power consumption, [kWh]
- E_n : Nighttime power consumption, [kWh]
- E_{np} : Power consumption of pumps at the newly serviced building, [kWh]
- I_p : Rotation rate of the cooling water pump, [-]
- I_C : Rotation rate of the cooling tower fan, [-]
- P_d : Daytime energy cost rate, [yen/kWh]
- P_n : Nighttime energy cost rate at the nighttime, [yen/kWh]
- Q : Cooling load, [kW]
- Q_s : Thermal storage amount, [kW]
- T_{wb} : Wet bulb temperature, [$^{\circ}$ C]
- V : Evaluation variable, [kW]
- $a_1 \sim a_4, b_1 \sim b_3$: Fitted coefficients
- η : Proportion of the energy consumed by thermal storage machines to total energy, [-]

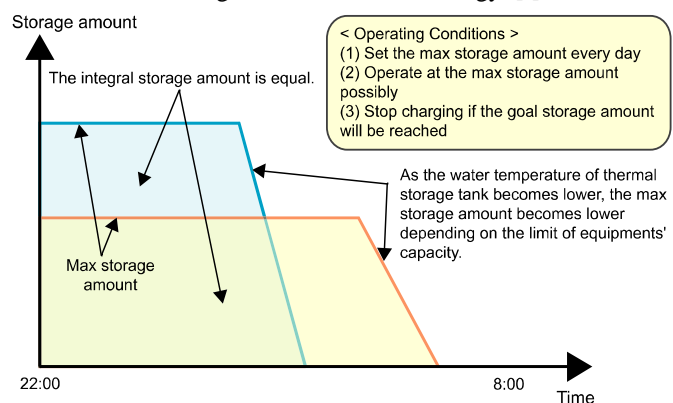


Figure 15: Control method for the thermal storage

Table 8: Simulation error of each equipment

	Chiller	Primary pump	Secondary pump	Charge pump	All model
Mean error [%]	8.1	12.1	9.6	3.5	6.7
RMSE [%]	13.1	15.4	13.2	6.7	10.3

Table 9 Total effects applying all the proposals

	(i)	(ii)	(iii)	(iv)	(v)	Total
Power consumption [%]	-	0.8	0.6	6.3	3.3	11.0
Energy cost [%]	-	0.8	0.6	5.6	1.2	8.2